Cent. Eur. J. Chem. • 7(4) • 2009 • 787–793
DOI: 10.2478/s11532-009-0069-0

VERSITA

Central European Journal of **Chemistry**

Activity and kinetics studies of *yeast* alcohol dehydrogenase in a reverse micelle formulated from functional surfactants

Research Article

Yun Zhang[1], Xirong Huang[1,2]*, Guanglei Ji[1], Ying Li[1], Weifeng Liu[2], Yinbo Qu[2]

[1]*Key Laboratory of Colloid & Interface Chemistry of the Education Ministry of China, Shandong University, Jinan, 250100, China*

[2]*State Key Laboratory of Microbial Technology of China, Shandong University, Jinan, 250100, China*

Received 1 March 2009; Accepted 28 April 2009

Abstract: Yeast alcohol dehydrogenase (YADH) showed substantial decrease in its catalytic activity due to the strong electrostatic interaction between the head groups of sodium bis(2-ethylhexyl) sulfosuccinate (AOT) and YADH in AOT reverse micelles. However, the catalytic activity of YADH in a nonionic reverse micellar interface (GGDE/TX-100) obtained from a functional nonionic surfactant N-gluconyl glutamic acid didecyl ester (GGDE) and Triton X-100 (TX-100) was higher than that in AOT reverse micelle under the respective optimum conditions. A comparison of the kinetic parameters showed that the turnover number k_{cat} in GGDE/TX-100 reverse micelle was 1.4 times as large as that in AOT reverse micelle, but the Michaelis constants in AOT reverse micelle for ethanol K_m^B was twice and for coenzyme NAD^+ K_m^A was 5 times higher than their counterparts in GGDE/TX-100 reverse micelle. For the conversion of ethanol, the smaller K_m^B and larger k_{cat} in GGDE/TX-100 reverse micelle resulted in higher catalytic efficiency k_{cat}/K_m^B. The stability of YADH in GGDE/TX-100 reverse micelle was also found to be better than that in AOT reverse micelle. They were mainly attributed to the absence of electric charge on the head groups of GGDE and TX-100 in the GGDE/TX-100 reverse micelle.

Keywords: *Alcohol dehydrogenase • Functional surfactant • Reverse micelle • Catalytic activity • Kinetic parameters*

1. Introduction

Alcohol dehydrogenase (ADH) is an NAD^+/NADH dependent oxidoreductase. It catalyzes the oxidation of alcohols as well as the reduction of aldehydes or ketones. Based on the fact that ADH is soluble in water whereas most of its substrates are insoluble in water, neither aqueous nor organic media are suitable for the ADH catalyzed reactions. Therefore, a microheterogeneous medium like a reverse micelle is the most apt environment for enzyme catalyzed reactions since it can dissolve the hydrophilic protein and the hydrophobic substrates. Many attempts have been made to carry out the enzymatic reactions in a reverse micellar medium [1-4]. Sodium bis(2-ethylhexyl) sulfosuccinate (AOT) is one such commercially available ionic surfactant that easily forms a stable reverse micelle. There are several reports on the catalytic performance of ADH in AOT reverse micelle [5-8] however, due to the strong electrostatic interaction between ADH and the head groups of AOT micelle, the catalytic activity of ADH in AOT reverse micelle was low. To alleviate the electrostatic interactions, some commercially available nonionic surfactants such as polyoxyethylene (4) lauryl ether were added to try and modify the interface of the AOT reverse micelle, and an enhancement in the activity was indeed observed [9]. However, it could not completely eliminate the effect of the electrostatic

* *E-mail: xrhuang@sdu.edu.cn*

interaction on ADH. Hence, we proposed to study the effect of N-gluconyl glutamic acid didecyl ester (GGDE), a two tailed nonionic surfactant with a sugar head group. In a reverse micelle formed by GGDE and Triton X-100 (TX-100), the catalytic activity of lignin peroxidase (LiP) was improved greatly as compared with in AOT reverse micelle [10]. It has been previously reported that sugar can stabilize the structure of ADH [11] hence to demonstrate the advantage of the functional nonionic surfactant for the full expression of the ADH activity in reverse micelles, the catalytic activity and kinetic parameters of *yeast* alcohol dehydrogenase (YADH) in both GGDE/TX-100 and AOT reverse micelles were studied and compared using ethanol as a substrate.

2. Materials and methods

2.1. Apparatus and reagents

UV-visible spectrophotometer (UV-2550) and its temperature-controlling accessories were products of Shimadzu Co. at Suzhou.

Triton X-100 (TX-100, Ultra) and AOT (99%) were purchased from Sigma-Aldrich Co.; nicotinamide adenine dinucleotide (NAD^+) was purchased from Shanghai Shenggong Bioengineering Co.; other reagents (domestic products) were of analytical grade. Triple distilled water was used throughout the experiments.

The alcohol dehydrogenase from *baker's yeast* (YADH, 451 U mg^{-1}) was purchased from Sigma-Aldrich Co. The concentration of YADH was calibrated based on its absorbance at 280 nm (ε_{YADH} = 189 L $mmol^{-1}$ cm^{-1}) [12].

The synthesis of nonionic surfactant GGDE and the pseudo ternary phase diagram of GGDE/TX-100-cyclohexane-H_2O were reported in our previous paper [10].

2.2. Analytical methods

In this paper, all concentration values were based on the overall volume of a reverse micellar solution. Data obtained experimentally were an average of three replicates. All experiments were carried out at 25°C.

2.2.1. Determination of the activity of YADH in GGDE/TX-100 reverse micelle

A certain amount of GGDE + TX-100 was first added into a vial containing an aliquot of cyclohexane, and then an aliquot of glycine-NaOH (50 mmol L^{-1}) buffer solution of a given pH was added. The mixture was sonicated for several minutes, resulting in a clear GGDE/TX-100 reverse micelle.

The above GGDE/TX-100 reverse micelle (0.5 mL) was added into a preheated quartz cuvette (1 cm long) and aliquots of absolute ethanol and YADH stock solution (35 μmol L^{-1}) were added. If necessary, additional buffer solution was added to change the molar ratio of water to surfactant (ω_0). Finally, NAD^+ stock solution (75 mmol L^{-1}) was added to initiate the YADH catalyzed oxidation of ethanol. After thorough mixing, a plot of absorbance (A) at 340 nm *versus* time (t) was recorded. The initial rate (υ_0) was calculated from the linear part of the A-t curve (ε_{NADH} = 6220 L mol^{-1} cm^{-1}) [8]. The catalytic activity of YADH was expressed as the initial rate of the YADH catalyzed oxidation of ethanol. Unless specified otherwise, the final concentrations of GGDE, TX-100, C_2H_5OH, YADH and NAD^+ were fixed at 40 mmol L^{-1}, 40 mmol L^{-1}, 68 mmol L^{-1}, 0.14 μmol L^{-1} and 0.30 mmol L^{-1}, respectively.

2.2.2. Determination of the activity of YADH in AOT reverse micelle

First, a stock solution of 100 mmol L^{-1} AOT in isooctane was prepared, then 0.5 mL of the stock solution was mixed in a 1 cm long preheated quartz cuvette with an aliquot of Tris-HCl (50 mmol L^{-1}) buffer solution of a given pH (its volume was determined by subtracting the volume of YADH and NAD^+ stock solutions from the total water volume calculated based on ω_0). After that, aliquots of absolute ethanol and YADH stock solution (35 μmol L^{-1}) were added. Finally, NAD^+ stock solution (75 mmol L^{-1}) was added to initiate the reaction. After thorough mixing, a plot of absorbance (A) at 340 nm *versus* time (t) was recorded. The initial rate (υ_0) was calculated from the linear part of the A-t curve (ε_{NADH} = 6220 L mol^{-1} cm^{-1}). The catalytic activity of YADH was expressed as the initial rate of the YADH catalyzed oxidation of ethanol. Unless specified otherwise, the final concentrations of AOT, C_2H_5OH, YADH and NAD^+ were fixed at 100 mmol L^{-1}, 68 mmol L^{-1}, 0.14 μmol L^{-1} and 0.30 mmol L^{-1}, respectively.

2.2.3. Determination of kinetic parameters

The YADH catalyzed oxidation of ethanol by NAD^+ obeyed an ordered mechanism [13]. The general rate equation can be expressed as:

$$\frac{1}{\upsilon_0}=\left(\frac{K_m^A}{V_{max}}+\frac{K_s^A K_m^B}{V_{max}[C_2H_5OH]}\right)\frac{1}{[NAD^+]}+\left(\frac{1}{V_{max}}+\frac{K_m^B}{V_{max}[C_2H_5OH]}\right) \quad (1)$$

where υ_0 is the initial rate of the ethanol oxidation; K_m^A, K_m^B are Michaelis constants for NAD^+ and ethanol, respectively; K_S^A is the dissociation constant of YADH-NAD^+; V_{max} is the maximum reaction rate. The kinetic parameters including the turnover number k_{cat} and the catalytic efficiency k_{cat}/K_m^B could be obtained in a normal way.

2.2.4. Stabilities of YADH in GGDE/TX-100 and AOT reverse micelles

A stock solution of YADH in GGDE/TX-100 ([GGDE] = [TX-100] = 40 mmol L^{-1}, ω_0 = 28, pH = 10.4 (glycine-NaOH)) or AOT ([AOT] = 100 mmol L^{-1}, ω_0 = 30, pH = 8.0 (Tris-HCl)) reverse micelles was first prepared and then kept in a water bath at 25°C. At given time intervals, an aliquot of YADH stock solution was taken out and mixed with preheated GGDE/TX-100 or AOT reverse micelles containing NAD^+ and ethanol. After that, a plot of absorbance (*A*) at 340 nm *versus* time (*t*) was recorded. The initial rate (υ_0) was calculated from the linear part of the *A*-*t* curve (ε_{NADH} = 6220 L mol^{-1} cm^{-1}). The final concentrations of C_2H_5OH, YADH and NAD^+ were 68 mmol L^{-1}, 0.14 μmol L^{-1} and 0.30 mmol L^{-1}, respectively.

3. Results and Discussion

3.1. Catalytic activity of YADH in different reverse micelles

3.1.1. Effect of ω_0

Fig. 1 showed the effect of ω_0 on the initial rate of the YADH catalyzed oxidation of ethanol. For curve A, no data were obtained at larger ω_0 due to the phase separation. In the ω_0 range studied, the initial rate both increased with the increase of ω_0; but the increment of the initial rate in GGDE/TX-100 reverse micelle was larger than that in AOT reverse micelle. In AOT reverse micelle, the initial rate first increased with the increase of ω_0 and then leveled off, which was similar to that reported elsewhere [14]. The optimum ω_0 in GGDE/TX-100 reverse micelle located at ca. 28, so a ω_0 value of 30 was selected as an optimum in AOT reverse micelle.

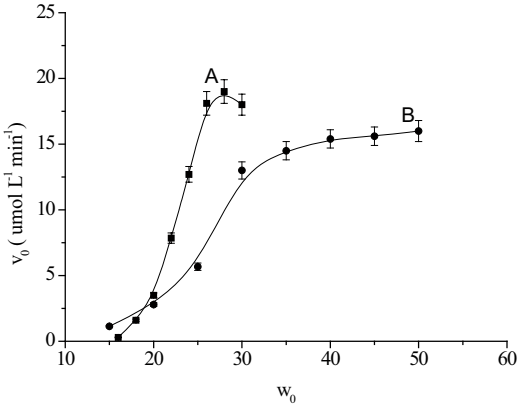

Figure 1. Effect of ω_0 on the catalytic activity of YADH in the GGDE/TX-100 mixed reverse micelle (pH = 10.1, A) and AOT reverse micelle (pH = 8.0, B).

3.1.2. Effect of pH

The effect of buffer pH on the catalytic activity of YADH is shown in Fig. 2. To our surprise, the two curves were quite different. In GGDE/TX-100 reverse micelle, the initial rate increased with the increase of the buffer pH (50 mmol L^{-1} glycine-NaOH) over the 8.6-10.4 pH range studied. Higher pH ranges were not studied since GGDE is prone to hydrolysis. In the AOT reverse micelles, the effect of the buffer pH (50 mmol L^{-1} Tris-HCl) on the YADH activity was studied over the pH range of 7.3-8.8. The pH profile was a bell-shaped curve with an optimum at pH 8.0.

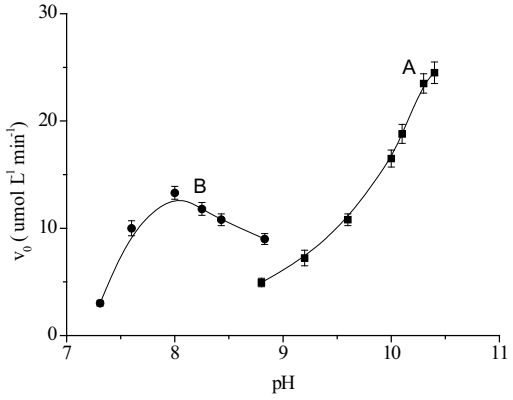

Figure 2. Effect of pH on the catalytic activity of YADH in the GGDE/TX-100 mixed reverse micelle (ω_0 = 28, A) and AOT reverse micelle (ω_0 = 30, B).

3.2. Kinetic parameters in different reverse micelles

Fig. 3 is a double reciprocal plot of the initial rate *vs.* the concentration of NAD^+ at different C_2H_5OH concentrations. Fig. 4 is the secondary replot of the intercepts and slopes of the double reciprocal lines in Fig. 3 *vs.* the corresponding inverse concentration of C_2H_5OH in GGDE/TX-100 reverse micelle. Figs. 5 and 6 are the corresponding plots in AOT reverse micelle. In the two media, both the primary and secondary plots were linear over the concentration ranges of 0.06-0.3 mmol L^{-1} for NAD^+, 10-50 mmol L^{-1} for ethanol. Based on the intercepts and slopes of lines in Fig. 4 or Fig. 6, the kinetic parameters K_m^A, K_m^B and V_{max}could be figured out. These data, together with k_{cat} and k_{cat}/K_m^B, are listed in Table 1. For comparison, the corresponding parameters in aqueous buffer solution are also given in Table 1.

Table 1. Kinetic parameters for YADH catalyzed oxidation of C_2H_5OH in GGDE/TX-100 and AOT reverse micelles.

kinetic parameters	GGDE/TX-100	AOT	Buffer*
K_m^A (mmol L^{-1})	0.0678	0.367	0.0445
K_m^B (mmol L^{-1})	11.0	19.9	1.21
V_{max} (μmol L^{-1} min^{-1})	45.5	33.3	94.3
k_{cat} (min^{-1})	325	238	674
k_{cat}/K_m^B ($mmol^{-1}$ L min^{-1})	29.5	12.0	557

* *pH = 8.8, 50 mmol L^{-1} Tris-HCl buffer*

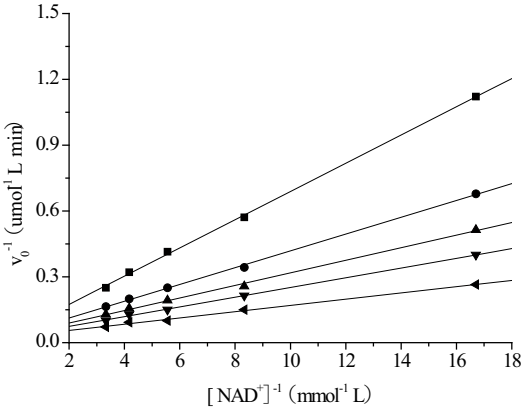

Figure 3. Double reciprocal plot of the initial rate *vs.* the concentration of NAD^+ at different C_2H_5OH concentrations in GGDE/TX-100 reverse micelle. ω_0 = 28, pH=10.4 and [C_2H_5OH] = 10 (■), 20 (●), 25 (▲), 30 (▼), 40 (◀) mmol L^{-1}.

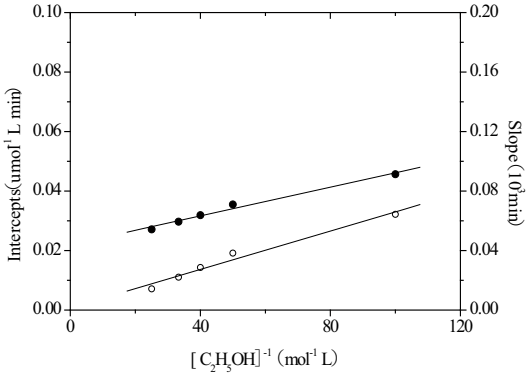

Figure 4. Secondary replot of the intercepts (●) and slopes (○) of the fitted lines in Fig. 3 *vs.* the corresponding inverse concentrations of C_2H_5OH.

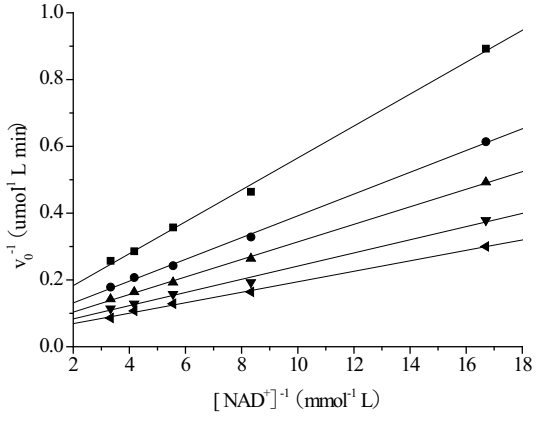

Figure 5. Double reciprocal plot of the initial rate *vs.* the concentration of NAD^+ at different C_2H_5OH concentrations in AOT reverse micelle. ω_0 = 30, pH=8.0 and [C_2H_5OH] = 10 (■), 20 (●), 30 (▲), 40 (▼), 50 (◀) mmol L^{-1}.

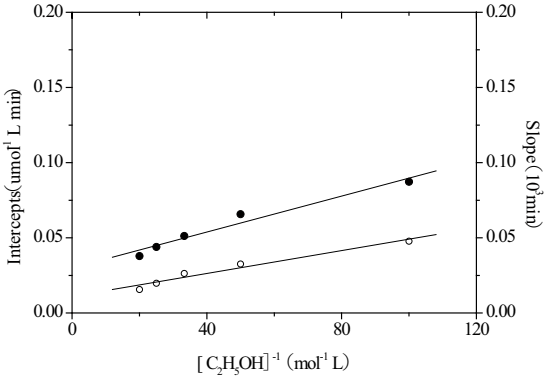

Figure 6. Secondary replot of the intercepts (●) and slopes (○) of the fitted lines in Fig. 5 *vs.* the corresponding inverse concentrations of C_2H_5OH.

3.3. Stabilities of YADH in different reverse micelles

The time-dependent activities of YADH (expressed as percentage with the original activity being 100%) in GGDE/TX-100 or AOT reverse micelles are shown in Fig. 7. The residual activity of YADH decreased rapidly in initial period and 10 h later, it approached a steady value. This behavior was quite similar to that reported by Chen *et al*. [9]. The steady value in GGDE/TX-100 reverse micelle (ca. 20%) was 2 times as large as that in AOT reverse micelle (ca.10%), indicating that GGDE/TX-100 reverse micelle was more favorable for YADH to retain its activity.

A literature survey indicated that there were several reports on the studies of the catalytic performance of YADH in AOT reverse micelles, but the results were

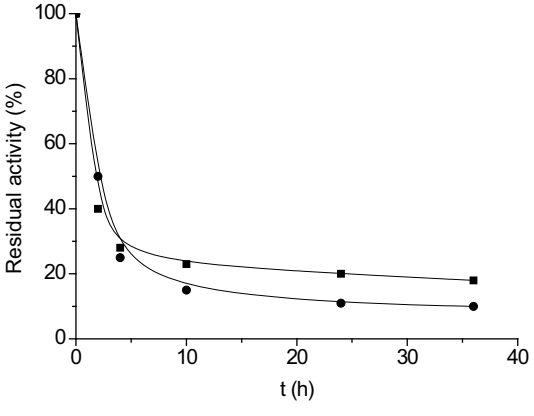

Figure 7. Time-dependent residual activities of YADH in GGDE/TX-100 reverse micelle (■) and AOT reverse micelle (●).

quite varied [5,6]. For comparison, we also studied the catalytic activity and kinetic parameters in AOT reverse micelle. It is worth a mention that the partition of the substrates (NAD^+ and ethanol) in a reverse micelle was not taken into account here because of their excellent solubility in water.

It is known that ω_0 plays an important role in the expression of catalytic activity of an enzyme. Before reaching the maximum value, the initial rate in the GGDE/TX-100 reverse micelle was much more sensitive to the ω_0 value than that in AOT reverse micelle. In the ω_0 range of 20-28, the initial rate in the GGDE/TX-100 reverse micelle was much larger than the counterpart in AOT reverse micelle. These phenomena could be explained using size-fit and the interfacial electrostatic interaction principles. With the increase of ω_0, the inner water pool of both reverse micelles increased in size. When the size of the pool matched the size of YADH, a high catalytic activity of YADH was observed. The radius of YADH was calculated to be ca. 3.7 nm based on its molecular weight (150,000D) and the hydrodynamic radius of the AOT reverse micelle at ω_0 = 30 was ca. 4.9 nm [15]. The size-fit principle fitted well for AOT reverse micelle. Apparently, the principle could not be applied for GGDE/TX-100 reverse micelle, because the hydrodynamic radius of the GGDE/TX-100 reverse micelle at ω_0 = 28 was measured to be ca. 18 nm [10]. However, if the big head groups of GGDE and TX-100 were taken into account, the size-fit principle was then reasonable. Owing to the absence of strong electrostatic interactions between the head group of surfactants and YADH in the GGDE/TX-100 reverse micelle, the increment of the catalytic activity was larger than the counterpart in AOT reverse micelle.

Since the YADH catalyzed oxidation of ethanol was accompanied by a proton transfer the acidity of the medium was an important factor for the expression of the catalytic activity of YADH. Determination of the pH in the water pool of the reverse micelle was difficult, so the pH of the stock buffer solution instead of that of the water pool was used for discussion [16]. The effect of buffer pH on the catalytic activity of YADH is shown in Fig. 2. The pH profiles were quite different. In AOT reverse micelle, the initial rate at the optimum pH of 8.0 was much lower than that in GGDE/TX-100 reverse micelle at pH 10.4 (which was taken as the optimum pH in GGDE/TX-100 reverse micelle). It is worth a mention that the buffer components were not responsible for the decrease of the YADH catalytic activity in AOT reverse micelle because the initial rate remained almost unchanged when different buffer (50 mmol L^{-1} glycine-NaOH buffer solution) of a same pH value (8.8) was used. The phenomenon that the two profiles were quite different could be explained on the basis of the electrostatic interaction between YADH and surfactants. YADH is an acidic protein with an isoelectric point (pI) of ca. 5.4 [12] therefore, when the pH of the buffer solution is higher than the pI, YADH is negatively charged. Moreover, the negative charges increases with increase in the pH value. Therefore, the electrostatic interaction between YADH and the head group of AOT becomes stronger with increase of pH in AOT reverse micelle hence, a higher pH is inappropriate for full expression of the YADH catalytic activity in AOT reverse micelle. In GGDE/TX-100 reverse micelle, however, there existed no such strong electrostatic interaction. Thus, higher pH was conducive to a full expression of the catalytic activity of YADH.

The above phenomenon was also correlated with the YADH catalyzed reaction mechanism and the kinetic parameters [17-19]. It has been reported that the dissociation of YADH-NADH complex was a rate-limiting step in the presence of excess reactants (relatively to the respective Michaelis constant). Moreover, the dissociation of NADH itself was pH-dependent. The dissociation degree increased with an increase in the pH value of the buffer. Therefore, the initial rate increased monotonously with increasing pH. However, when the concentration of NAD^+ or C_2H_5OH was lower than the respective Michaelis constant, the step of the conversion of ethanol to acetaldehyde became rate-limiting and a maximum is reached in the plot of the initial rate *versus* pH. In our experiments, the concentration of ethanol (68 mmol L^{-1}) was much higher than the corresponding K_m^B in both GGDE/TX-100 and AOT reverse micelles (Table 1); the concentration of NAD^+ (0.30 mmol L^{-1}) was also higher than the K_m^A in GGDE/TX-100 reverse micelle, but a little lower than the K_m^A in AOT reverse micelle. Thus, two different pH profiles were seen.

When the turnover number k_{cat} in both reverse micelles were compared with that in aqueous solution, we found that the interface formed by AOT or GGDE/TX-100 did have a negative effect on the catalytic activity of YADH. As shown in Table 1, the k_{cat} in the aqueous solution was bigger than that in the two reverse micellar solutions. This phenomenon should be ascribed to the conformational change of YADH perturbed by the interfaces. The fact that the k_{cat} value in GGDE/TX-100 reverse micelle was ca. 1.4 times as large as that in AOT reverse micelle indicated that the perturbation caused by AOT was larger than that by GGDE/TX-100 due to the lack of electrostatic interactions in reverse micellar medium formed by the latter. The conformational change of YADH also reduced its affinity to the substrates. The Michaelis constant of ethanol K_m^B in the two reverse micelles was several times (9 for GGDE/TX-100 and

16 for AOT) as large as that in the aqueous solution. Even so, the K_m^B in GGDE/TX-100 reverse micelle was still lower than that in AOT reverse micelle. This result indicated an increased affinity of YADH for ethanol in GGDE/TX-100 reverse micelle. Ethanol being a neutral molecule, the difference in K_m^B cannot be ascribed to its partition in the pseudophase. The absence of the electrostatic interaction between GGDE/TX-100 and YADH should be responsible for the further decrease of K_m^B in GGDE/TX-100 reverse micelle. The same explanation was applied to the Michaelis constant of NAD^+, K_m^A. Table 1 shows that the affinity of YADH for NAD^+ in GGDE/TX-100 reverse micelle approached that in the aqueous solution, but was much stronger than that in the AOT reverse micelle. The weak affinity of YADH for NAD^+ in AOT reverse micelle was correlated with the negative charge on the head group of AOT. The strong electrostatic attraction between the head group of AOT and NAD^+ reduced the ability of NAD^+ to bind to YADH.

Due to the smaller K_m^B and bigger K_{cat} as mentioned above, the catalytic efficiency of YADH k_{cat} / K_m^B in GGDE/TX-100 reverse micelle was approximately 2.5 times as large as that in AOT reverse micelle. Also we found that the stability of YADH in GGDE/TX-100 reverse micelles was better than that in AOT reverse micelles. It followed that the nonionic surfactant GGDE/TX-100 was better than AOT for the full expression of the YADH catalytic activity in reverse micelles.

4. Conclusions

The present studies indicated that there exists an interaction between YADH and the interface formulated by GGDE/TX-100 or AOT, which induced a conformational change of YADH, and therefore resulted in lower k_{cat} in both reverse micellar media when compared to the aqueous medium. The k_{cat} in AOT reverse micelle was lower than that in GGDE/TX-100 reverse micelle because of the negative charges on the head group of AOT. The same also resulted in bigger K_m^B and K_m^A in AOT reverse micelle than in GGDE/TX-100 reverse micelle. Unlike ethanol, NAD^+ is a cation, thereby, the strong electrostatic attraction between the negatively charged head groups of AOT and NAD^+ made the K_m^A in the AOT reverse micelle increase further. For the conversion of ethanol, the smaller K_m^B and bigger k_{cat} in GGDE/TX-100 reverse micelle resulted in higher k_{cat} / K_m^B. The stability test also showed that YADH hosted in GGDE/TX-100 reverse micelles was more stable than that in AOT reverse micelle. In short, the interface formulated by a mixture of the two tailed nonionic surfactant GGDE and TX-100 was better than that by AOT for the full expression of the catalytic activity of YADH in reverse micellar medium.

Acknowledgments

The authors gratefully acknowledge financial support from State Key Laboratory of Microbial Technology of China, the Natural Science Foundation of Shandong Province, the National Natural Science Foundation of China (30570014), and the National Basic Research Program of China (2007CB936602).

References

[1] K. Martinek, A.V. Levashov, N. Klyachko, Y.L. Khmelnitski, I.V. Berezin, Eur. J. Biochem. 155, 453 (1986)
[2] O. Bernhard, S. Reinhard, Adv. Biochem. Eng. Biotechnol. 75, 185 (2002)
[3] M.A. Biasutti, E.B. Abuin, J.J. Silber, Adv. Colloid Interface Sci. 136, 1 (2008)
[4] J. Rodakiewicz-Nowak, Top. Catal. 11/12, 419 (2000)
[5] S. Sarcar, T.K. Jain, A. Maitra, Biotechnol. Bioeng. 39, 474 (1992)
[6] D.H. Chen, H.H. Chen, T.C. Huang, J. Chem. Technol. Biotechnol. 64, 217 (1995)
[7] K.M. Larsson, P. Adlercreutz, B. Mattiasson, Eur. J. Biochem. 166, 157 (1987)
[8] S. Das, S. Mozumdar, A. Maitra, J. Colloid Interface Sci. 230, 328 (2000)
[9] D.H. Chen, M.H. Liao, J. Mol. Catal. B 18, 155 (2002)
[10] Y. Zhang, X.R. Huang, F. Huang, Y.Z. Li, Y.B. Qu, P.J. Gao, Colloids Surf. B 65, 50 (2008)

[11] M. Miroliaei, B. Ranjbar, H. Naderi-Manesh, M. Nemat-Gorgani, Enzyme Microb. Technol. 40, 896 (2007)
[12] J.E. Hayes, S.F. Velick, J. Biol. Chem. 207, 225 (1954)
[13] H. Yang, D.J. Kiserow, L.B. McGown, J. Mol. Catal. B 14, 7 (2001)
[14] H. Hirakawa, N. Kamiya, T. Yata, T. Nagamune, Biochem. Eng. J. 16, 35 (2003)
[15] S.L.A. Andrade, C.D. Brondino, E.O. Kamenskaya, A.V. Levashov, J.J.G. Moura, Biochem. Biophys. Res. Commun. 308, 73 (2003)
[16] R.E. Smith, P.L. Luisi, Helv. Chim. Acta 63, 2302 (1980)
[17] E. Silverstein, P.D. Boyer, J. Biol. Chem. 239, 3908 (1964)
[18] V. Leskovac, S. Trivic, B.M. Anderson, Eur. J. Biochem. 264, 840 (1999)
[19] F.M. Dickinson, G.P. Monger, Biochem. J. 131, 261 (1973)